

An alternating lock-down strategy for sustainable mitigation of COVID-19

Dror Meidan¹, Reuven Cohen¹, Simcha Haber¹ & Baruch Barzel^{1,2}

1. Department of Mathematics, Bar-Ilan University, Ramat-Gan 52900, Israel

2. Gonda Multidisciplinary Brain Research Center, Bar-Ilan University, Ramat-Gan 52900, Israel

- **Correspondence:** Baruch Barzel, baruchbarzel@gmail.com

Lacking a drug or vaccine, our current strategy to contain the COVID-19 pandemic is by means of social distancing, specifically mobility restrictions and lock-downs. Such measures impose a hurtful toll on the economy, and are difficult to sustain for extended periods. The challenge is that selective isolation of the sick, an often viable and effective strategy, is insufficient against COVID-19, due to its relatively long incubation period, in which exposed individuals experience no symptoms, but still contribute to the spread. Here we propose an alternating lock-down strategy, in which at every instance, half of the population remains under lock-down while the other half continues to be active, maintaining a routine of weekly succession between activity and lock-down. All symptomatic individuals continue to remain in isolation. Under this regime, if an individual was exposed during their active week, by the time they complete their lock-down they will already begin to exhibit symptoms. Hence this strategy isolates the majority of exposed individuals during their asymptomatic phase. We find that this strategy not only overcomes the pandemic, but also allows for some level of flexibility, withstanding a fraction of defectors or essential workers that remain continuously active. We examine our strategy based on current epidemiological models with parameters relevant for COVID-19. We wish, however, following this communication, to further test and fine-tune our scheme based more refined data, and assess its actual effectiveness.

Note from the authors. *In light of the imminence of the matter, we have decided to publish this report, even in its preliminary form, forgoing the scientific instinct of scrutiny and reservedness. We will continue to refine and retest our results and update this report on the go. We also welcome feedback, comments, questions or advice that can help further test or improve our proposed strategy.*

Overview

As we battle the virulent spread of COVID-19 we seek efficient strategies to mitigate its global impact. Lacking therapeutic interventions, such as drugs or vaccines, we resort to social distancing, aimed primarily at lowering the reproduction rate R_0 and *flattening the curve*, *i.e.* reducing the total number of infected individuals, while spreading their infection over an extended period [1–3]. Such measures are designed to avoid shocking the health-care system, reducing the medical burden, and slowing its onset, hence keeping it within the bounds of the system’s capacity. To achieve this many countries have imposed social restrictions [3], from complete lock-downs, to severe mobility constraints, indeed, slowing down the viral propagation, but at the same time, taking a severe toll on social and economic stability. Most current projections on COVID-19 indicate that such social distancing policies must be put in place for extended periods (typically months) to avoid reemergence of the epidemic once lifted [4]. This, however, may be unsustainable, as individual social and economic needs will, at some point surpass the perceived risk of the pandemic.

Another challenge, specific to COVID-19, is its incubation period, estimated at ~ 5 days on average

[5, 6], and, at times observed to be as long as two weeks. During this period *exposed* individuals are asymptomatic, but may still spread the virus - essentially behaving as *invisible spreaders* that continue to interact. Under such circumstances it is difficult to selectively isolate the sick, as the asymptomatic spreaders continue to infect the population [3]. This, we believe, may be the reason that, despite our seclusion of the infected individuals, we continue to witness a rapid growth in the disease coverage - further strengthening the need for an economically hurtful population wide lock-down.

We, therefore, seek a balanced mitigation strategy, that is, on the one hand economically viable and sustainable for an extended period, and, on the other hand allows us to bypass the challenge posed by the invisible spreaders. We arrived at an efficient policy of an *alternating lock-down*, based on two principals: (i) Complete isolation of the infected individuals, as already practiced at present [3]; (ii) Partitioning of the remaining population into two groups that undergo weekly successions of lock-downs and routine activity. Hence while group 1 remains active, group 2 stays at home and vice versa. This allows half of the population to remain active at any instance, by enabling each individual to participate in the work force and partake in social activities for half of the time. Of course, at all times, infected individuals, who already exhibit COVID-19 symptoms should remain in isolation, regardless of their group affiliation. It is also crucial that the partition is at a household level, rather than per individual (*e.g.*, based on address), such that all people sharing the same habitat are in the same group, avoiding inter-group spillover.

This strategy of alternating lock-downs limits social mixing, while providing an outlet for people to sustain their economic and social routines. At the same time it treats one of the main obstacles for COVID-19 mitigation - the 5 day incubation period. Indeed, isolating people for, *e.g.*, an entire week after they have been socially active, ensures that the majority of the exposed individuals are confined to their homes. To understand this consider an individual in Group 1 who was active during week 1, and therefore might have been infected. According to the proposed routine, this individual will anyway enter lock-down in week 2, and hence will be isolated precisely during their suspected incubation period. If, at the end of week 2 they remain asymptomatic, most chances are that they are, in fact, healthy, and can, therefore, resume activity at week 3 according to the planned routine. Conversely, if they do develop symptoms during their lock-down week, they must remain in isolation, similar to all symptomatic individuals. *Hence, the weekly succession is in resonance with the natural COVID-19 disease cycle, and in practice, leads to isolation of the majority of invisible spreaders.*

Our numerical analysis indicates that this strategy, if implemented successfully, leads to an immediate and rapid decline in infection levels, effectively pushing the system from the pandemic state ($R_0 > 1$) to the healthy state ($R_0 < 1$) [9]. This is despite the potential variability in incubation times, in which a fraction of individuals may remain asymptomatic for more than the typical 5 days. We also examine the case of imperfect implementation by including a percentage of social defectors who violate their lock-down terms and remain active at all times. We find that our strategy is generally robust against such violations. As defection levels increase, however, the steep decline of the epidemic is replaced by a more minor reduction in R_0 and, hence, an effective flattening of the curve. Both results represent desirable mitigation outcomes.

Analysis

Modeling the COVID-19 epidemic. We consider a Susceptible-Exposed-Infected-Recovered (SEIR) model [7], in which the population is divided into four states: S , available to contract the disease; E , exposed individuals that are asymptomatic, yet infectious; I , infected and R , recovered. We assume that, even without employing major social distancing measures, such as lock-downs or quarantines, the infected individuals (I), who exhibit symptoms, are generally isolated, and hence do not contribute to the spread. Therefore, the spreaders are the exposed individuals (E), who continue to interact with their network of acquaintances, unaware that they are infectious. Under these conditions the transitions between the S, E, I, R states follow



such that upon infection susceptible individuals enter an incubation period, in which they are at the exposed state E .

In the standard implementation of the SEIR model Eq. (2), capturing the transition from E to I , is simulated via a Poissonian process, in which exposed individuals transform into the infected state at a constant rate. This leads to an exponential decay in $E(t)$ that begins upon infection, representing a memory-less process, whose probability is independent of the time since exposure. In reality, however, incubation has a typical time-scale, and therefore, the transition to I occurs preferably around that time after initial exposure. Hence, in our implementation, to model the incubation period more realistically, we assume that incubation times follow an arbitrary distribution $g(t)$, describing the probability density for an individual to remain asymptomatic for a period $t' \in (t, t + dt)$. The density $g(t)$ captures both the average incubation time, as well as its potential variability across the population. Denoting the fraction of individuals in each state by $S(t), E(t), I(t)$ and $R(t)$, *i.e.* $S(t) + E(t) + I(t) + R(t) = 1$, we can model transitions (1) - (3) as shown in **Appendix A**.

In Fig. 1a we show the results of the SEIR dynamics, starting from a fully susceptible population penetrated by a small seed of infectious individuals, *i.e.* $S(t = 0) = 1 - 10^{-3}$, $E(t = 0) = 10^{-3}$, $I(t = 0) = 0$ and $R(t = 0) = 0$. This captures the evolution of the unmitigated epidemic, absent any intervention policy, aside from isolation of the sick, *i.e.* people in the I state. We set the parameters to match the observed epidemiological data obtained for COVID-19: for the incubation period we set $g(t) \sim N(\mu, \sigma^2)$, a normal distribution with mean $\mu = 5$ days and $\sigma = 0.5$ [5, 6]. Assuming an average 11 day recovery from the onset of symptoms [8], we set $\alpha = 0.09$ (days $^{-1}$). To evaluate the infection rate β we collected data capturing all diagnosed cases in Israel over a period of 20 days, providing an empirical observation of $I(t)$. We find that the diagnosed cases can be well-approximated by an exponential inflation of the form $I(t) \sim e^{kt}$, with $k \approx 0.3$ days $^{-1}$. Setting $\beta = 0.32$ in (1) provides the desired exponential increase that best concurs with the observed data (Fig. 1a).

Using these coefficients we obtained a projection of the expected evolution of the epidemic (Fig. 1b). We extract three crucial parameters, directly quantifying the severity of the spread: First is

$$R_\infty = R(t \rightarrow \infty), \quad (4)$$

designed to capture the overall fraction of infected individuals throughout the spreading period. Our results indicate that, unmitigated, COVID-19 will lead to an order of $R_\infty \approx 0.65$, *i.e.* $\sim 65\%$ total infection (purple). Next we seek

$$I_{\text{Peak}} = \max_{t=0}^{\infty} (I(t)), \quad (5)$$

capturing the fraction of infected individuals at the peak of the spread. If I_{Peak} is large, the health care system resources may be stretched beyond capacity. Our results project a peak infection of $I_{\text{Peak}} \approx 0.25$ (yellow). Finally, to quantify the duration of the epidemic spread we measure the time T for $I(t)$ to decay below η following the peak infection, namely

$$I(t \geq T) < \eta. \quad (6)$$

Here, setting $\eta = 10^{-3}$, we estimate the duration of the spread at $T \approx 120$ days, a projected four month or more of sustained pandemic state.

A proper mitigation strategy aims to eliminate the spread, or, at the least, *flatten* the $I(t)$ curve: reduce R_∞ and I_{Peak} , to ensure a manageable level of infection across the population. At the same time, however, we wish to avoid over-extending T , to allow a return to normalcy within a reasonable time-frame. Below we examine the behavior of the SEIR model under the alternating lock-down regime.

Mitigation

Weekly alternating lock-down. Our mitigation begins at time $t = t_0$, at which point the state of the system is given by $S(t_0), E(t_0), I(t_0)$ and $R(t_0)$. With this initial condition, we partition the population randomly into two equal groups 1 and 2, which are instructed to alternate in succession between a complete lock-down and regular activity. Individuals at the I state are instructed to always remain isolated, regardless of whether their group is in the active phase or on lock-down. The lock-down/activity periods are set to $\tau = 7$ (days), *i.e.* weekly shifts between the groups. This time scale is selected in order to approximately resonate with the disease average incubation period of ~ 5 days. Hence, if incubation is longer, one must set longer shifts. In our simulations we also allow for variability in incubation period, as captured by the distribution $g(t)$, and quantified by the variance σ^2 .

The level of cooperation in the society is captured by the fraction f of defectors, who despite being on lock-down continue their out of home activities. Hence, $f = 0$ represents a fully disciplined society, which abides by the lock-down rules, and $f = 1$ captures a defiant society, in which all individuals violate the lock-down. This fraction f may also capture a limited amount of essential workers who are officially exempt from the lock-down. Despite the presence of potential defectors or essential workers, it remains crucial that individuals exhibiting symptoms (I state) continue to be isolated. Indeed, while asymptomatic E state individuals may have the audacity to defect, we assume that once they become symptomatic, even they will choose to abide by the social distancing norms. In **Appendix B** we construct the relevant equations to realize this mitigation strategy.

To err on the safe side, we examine the impact of the alternating lock-downs in the absence of any other preventive measures, namely, we assume that the population continues its pre-COVID-19 behavioral norms, with the only difference being the bi-weekly lock-down routine. Hence all the epidemiological parameters obtained in our analysis of the unmitigated spread remain unchanged - specifically the infection rate, which we continue to set at $\beta = 0.32$. Starting our mitigation at $t_0 = 10$ days we observe that the infection curve $I(t)$ changes dramatically (Fig. 2a, blue, see inset). The peak infection, I_{Peak} (5), as well as the total infection, R_∞ (4), become orders of magnitude lower compared to the unmitigated spread (grey). Responding at later times (blue - red gradient) increases I_{Peak} , however, for all response times, ranging from $t_0 = 10$ to 50 days, the alternating lock-down consistently leads to an immediate and rapid decay of the epidemic.

Next, we examine the impact of defectors, f , from 10–30% defection rate (Fig. 2b - d). We find that even under a 15% defection rate our strategy practically eliminates the spread, observing a dramatic reduction in infection. Setting $f = 0.3$, we begin to observe a decline in the performance of our strategy, as now the viral spread continues, albeit at a lower rate. Indeed, under these conditions instead of fully eliminating the spread, the alternating lock-down scheme allows to merely flatten the curve. *Hence, in all scenarios, alternating lock-down achieves efficient mitigation, either fully blocking the spread in a cooperative regime, or, at the least, if cooperation levels are insufficient, flattening it to manageable levels.*

To examine the performance of our strategy more systematically we measured the three parameters, R_∞ , I_{Peak} and T as appear in Eqs. (4) - (6), while gradually increasing the defection rate f (Fig. 2e - g). We find that the system undergoes a transition, similar to the pandemic transition, at a critical rate of defection, here observed at $f \approx 0.17$. Below this value, alternating lock-downs effectively push R_0 below unity, and hence *eliminate* the epidemic: $I(t)$ rapidly decays, and R_∞ and I_{Peak} both approach zero, similar to the behavior below the pandemic threshold [9, 10]. Above this defection level, our strategy no longer eliminates, but *flattens* the epidemic curve: $I(t)$ continues to grow, however R_∞ and I_{Peak} become smaller, equivalent to the effect of reducing R_0 . This transition is also observed in the behavior of T . Indeed in the elimination phase ($f < 0.17$) the epidemic rapidly decays within a short time, while under flattening ($f > 0.17$) the duration is extended, and T becomes large. In both regimes, however, successful mitigation is achieved - either eliminating or flattening the curve.

Another challenge to our strategy is the potential variability in the incubation period. This allows a fraction of people, whose asymptomatic phase is longer than average, to remain in the E state throughout their lock-down week, then continue to infect others as they resume activity. Our model accounts for such variability through $g(t)$ and its variance σ^2 . In Fig. 2h - j we examine the impact σ on our mitigation. Quite strikingly, we find that even extreme levels of heterogeneity in incubation time, with σ as high as 5 or 10 (namely, two times the mean), still have little impact on the performance of our strategy. In fact, under all values of σ the peak infection remains at a level of less than 1%. The only exception is when $t_0 = 50$, a late response in which $I(t)$ was already above 1%, and hence I_{Peak} reached, at its maximum level 3% (Fig. 2i, red). For the duration T we continue to observe a similar trend, where T is low under small σ , but becomes higher as σ is increased, and the $I(t)$ curve is flattened rather than eliminated. Overall, however, we find that our strategy is, by and large, insensitive to incubation time variability.

Taken together, we find that alternating lock-down is highly efficient, thanks to its resonance with the natural COVID-19 disease cycle. Under ideal conditions, *i.e.* $f, \sigma \rightarrow 0$ eliminates the disease within a single two week cycle, guaranteeing that all invisible spreaders remain locked down. Our results, however, indicate that its efficiency extends beyond that. The method is found to be robust both against imperfect implementation (large f) and against individual variability in incubation times (large σ). It should therefore be considered as a leading strategy, tailored for the mitigation of COVID-19.

Discussion

Alternating-lock-downs offer a sustainable strategy to overcome COVID-19. It allows to continue the socio-economic activity at a 50% rate, while mitigating the spread. We designed our strategy under the assumption of imperfect social compliance [11], allowing a defection fraction of f . We believe, however, that the weekly relief, allowing people an outlet to continue and be active half of the time, may, itself, increase cooperation levels. Indeed, while a complete lock-down is extremely stressful for the individual, the bi-weekly routine offered here relaxes the burden, and may encourage compliance. This also provides a degree of freedom to allow a certain level of *authorized defection*, *i.e.* a quota of essential workers that can be relieved from the lock-down periods.

In practice, we believe that the simplest implementation can be by regulating schools and workplaces. Each house-hold will be informed on its lock-down/active schedule, and in parallel workplaces and schools will only be allowed to operate in weekly fully partitioned shifts. Under such regulations the strategy has little dependence on social cooperation, as schools and employment will naturally drive the population between activity and inactivity. The only *enforcement* of the lock-down that will still be required is for recreational activities, beyond school and work. We believe that the pressure to defect for such activities is lower, and hence overall defection levels can be sustained well within the bounds of successful mitigation.

Our analysis assumes an incubation period that is of the order of a single week, specifically in our simulations, we set it at an average of 5 days. The rationale however is more general, and can be adapted to longer or shorter incubation times, simply by tuning the periodicity of the lock-down shifts, keeping them congruent with the natural cycle of the disease.

More broadly, we consider the fact that there is, inherently, some level of uncertainty regarding the disease parameters. We therefore assumed a worst case scenario, in which the infection rate during the active weeks is the same as that of the unmitigated spread. In practice, however, we expect many additional measures to be implemented in parallel to the lock-downs, such as extended testing for infections, and strict hygienic regulations at the workplace. At the least, we expect standard prophylactic behavior, such as avoiding contact or banning social gatherings, to be observed also during each group's active week. Such norms, that will continue until COVID-19 is fully mitigated, will further push down β , enhancing the effectiveness of our strategy even under higher f or σ .

Alternating lock-downs offers an additional crucial advantage, that, again - assuming worst case - we did not exploit in our simulations. Indeed, the fact that at each time point only half of the population is active, is, itself, an enhancer of prophylactic norms. With classrooms, public transport, offices and marketplaces at only half capacity, it becomes more natural to maintain social distancing, and reduce infectious interactions. Hence, our partition will further push down

the infection rate β , likely leading to an even better performance than reported in Fig. 2.

Our simulation results are based on a simplistic SEIR model, potentially overlooking much of the complexity and irregularity characterizing the spread in a real social setting. Moreover, while our modeling covers the epidemiological aspects of the strategy, it cannot advise on its practical implementation or on its economical viability. Finally, tested against real-time data of, *e.g.*, human mobility, will enable further fine-tuning of the proposed strategy. For example, partitioning into more groups, if possible, allowing extended activity periods, or changing the schedule from weekly to, *e.g.*, 10 days, etc. • *Therefore, we do not call for the immediate implementation of alternating lock-downs. We do, however, think that the potential merits of this scheme warrant its consideration as a leading strategy for mitigation of COVID-19. As we communicate this idea - we invite critique, and further examination of its applicability, and especially, call for testing it against real-time human interaction data, to fine-tune its implementation and assess its effectiveness.*

Data availability. All codes to reproduce, examine and improve our proposed analysis are available at <https://github.com/drormeidani/ALDCOVID19>.

-
- [1] C. Fraser, S. Riley, R.M. Anderson and N.M. Ferguson. *Proc. Natl. Acad. Sci. USA*, 101:6146, 2004.
 - [2] R.M. Anderson *et al.* Epidemiology, transmission dynamics and control of SARS: the 2002/2003 epidemic. *Phil. Trans. Roy. Soc. Ser. B*, 359:1091, 2004.
 - [3] R.M. Anderson, H. Heesterbeek, S. Klinkenberg and T.D. Hollingsworth. How will country-based mitigation measures influence the course of the COVID-19 epidemic? *The Lancet*, 395:10228, 2020.
 - [4] J. Hellewell *et al.* Feasibility of controlling COVID-19 outbreaks by isolation of cases and contacts. *Lancet Global Health*, 8:488, 2020.
 - [5] Q. Li *et al.* Early transmission dynamics in Wuhan, China, of novel coronavirus-infected pneumonia. *N Engl J. Med.*, 382:1199, 2020.
 - [6] WHO. Coronavirus disease (COVID-2019) situation report 30. 2020.
 - [7] R. Pastor-Satorras, C. Castellano, P. Van Mieghem and A. Vespignani. Epidemic processes in complex networks. *Rev. Mod. Phys.*, 87:925–958, 2015.
 - [8] L. Zou *et al.* SARS-CoV-2 viral load in upper respiratory specimens of infected patients. *N. Engl. J. Med.*, 382:1177, 2020.
 - [9] L. Hufnagel, D. Brockmann and T. Geisel. Forecast and control of epidemics in a globalized world. *Proc. Natl. Acad. Sci. USA*, 101:15124–9, 2004.
 - [10] A. Vespignani. Modelling dynamical processes in complex socio-technical systems. *Nature Physics*, 8:32–39, 2012.
 - [11] D. Cyranoski. What China's coronavirus response can teach the rest of the world. *Nature*, 579:479, 2020.

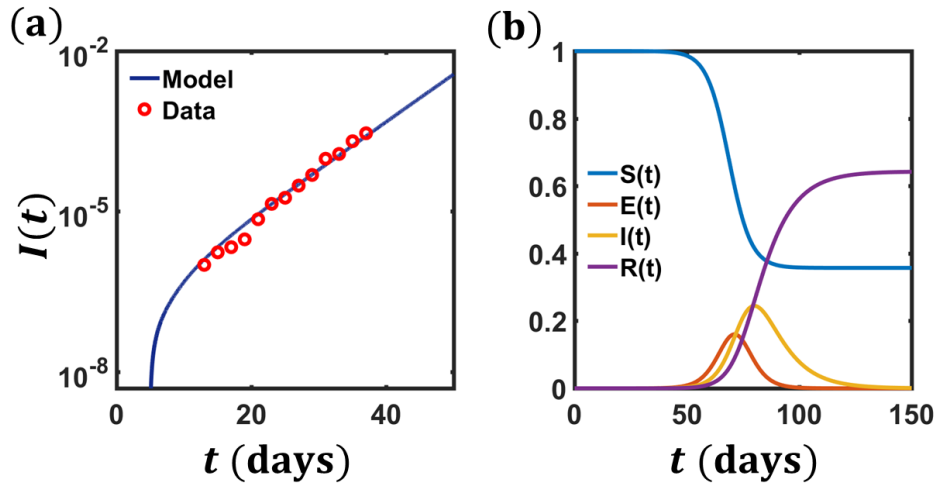


FIG. 1: **Modeling COVID-19.** (a) We collected data on the infection levels vs. time from the Israel Ministry of Health (circles). We observe an exponential increase at a rate of $\sim e^{0.3t}$, congruent with data collected in other locations. Our SEIR model (**Appendix A**) is found to be in good agreement with the observed exponential increase of $I(t)$ under the following parameters: $\alpha = 0.09, \beta = 0.32$ and $g(t)$ having a mean of $\mu = 5$ days. (b) Using this parameters we simulated the projected spread of COVID-19, lacking any preventive measures.

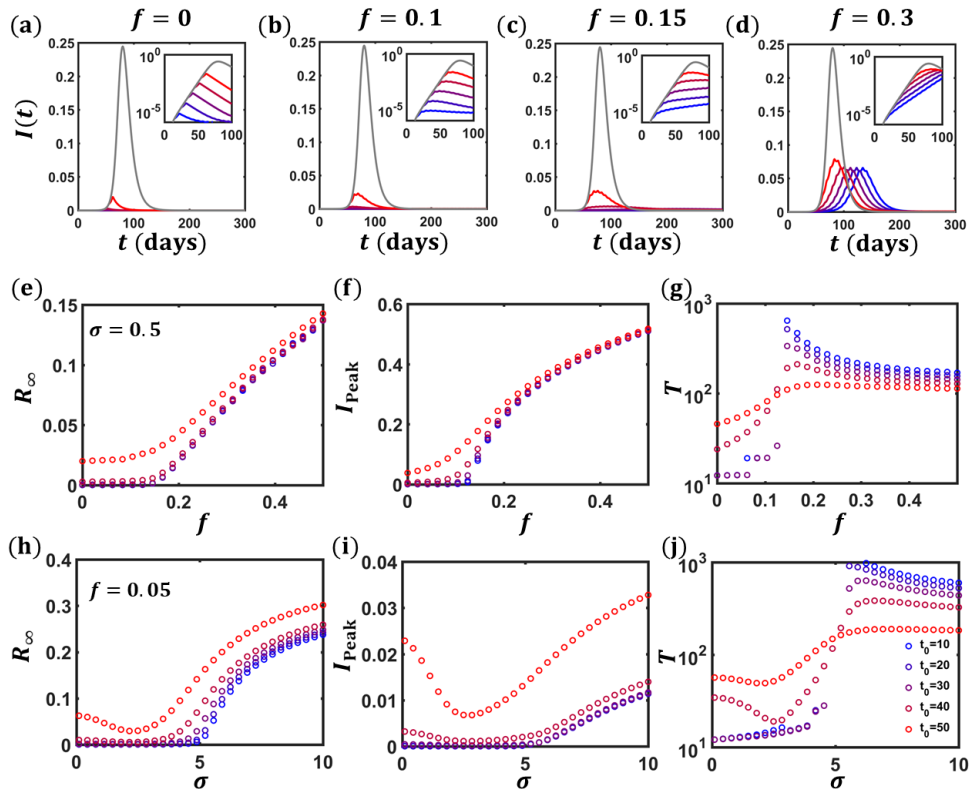


FIG. 2: **The impact of alternating lock-down.** (a) The infection $I(t)$ vs. t of the unmitigated epidemic (grey) and under our mitigation starting at $t_0 = 10$ days (blue). The epidemic is rapidly eliminated, to the extent that the blue curve is undecipherable. To observe it we include the log-scale representation (inset), showing that our mitigation reduces $I(t)$ by orders of magnitude. As our response time is increased (blue - red gradient, see legend in panel j), we observe higher infection levels. However, under all conditions alternating lock-downs rapidly eliminate the disease. (b) - (c) Similar results are obtained also under a 10–15% deflection level f . (d) For higher deflection $f = 0.3$, our strategy does not *eliminate* the disease, but rather reduces its reproduction rate R_0 and effectively, *flattens the curve*. (e) The overall infection R_∞ vs. f under different intervention times t_0 (blue - red gradient). We observe a transition, in which for $f < 0.17$ the disease is eliminated. Beyond this deflection rate, spread is suppressed, but not fully eliminated, *i.e.* flattened. (f) Similar results for I_{Peak} vs. f . (g) Duration T vs. f . For small f the mitigation is rapid (elimination). For large f , however, the overall duration is increased - an inevitable price of flattening the curve. (h) - (j) We measured the three parameters vs. the variability in incubation times σ . We find that our strategy is highly insensitive to σ , however for $\sigma > 5$, a rather extreme level of variability, duration becomes highly extended.

Appendix A. Modeling COVID-19

We consider a population of N individuals, of which $\mathbb{S}(t)$ are susceptible, $\mathbb{E}(t)$ are exposed, $\mathbb{I}(t)$ are infected and $\mathbb{R}(t)$ are recovered, hence $\mathbb{S}(t) + \mathbb{E}(t) + \mathbb{I}(t) + \mathbb{R}(t) = N$ for all t . The exposed individuals develop symptoms within a time t from exposure, extracted from the distribution $g(t)$. Therefore, the number of individuals that transition to the I state at time t depends on $d\mathbb{E}_+(t - t')$, namely the number of people added to the E state at an infinitesimal range dt around $t - t'$. This is driven by the process of exposure in Eq. (1), which translates to

$$\frac{d\mathbb{E}_+}{dt} = \beta\mathbb{E}(t)\frac{\mathbb{S}(t)}{N}, \quad (7)$$

proportional to the number of exposed individuals \mathbb{E} and to the probability \mathbb{S}/N to interact with a susceptible individual. Of all individuals infected around $t - t'$, a fraction $g(t')$ will transition to the I state at time t , and therefore the rate of reduction in \mathbb{E} (or contribution to \mathbb{I}) at time t is captured by

$$\mathbb{G}(t) = \int_0^t g(t')\beta\mathbb{E}(t - t')\frac{\mathbb{S}(t - t')}{N} dt'. \quad (8)$$

Equation (8) sums over all individuals exposed from $t = 0$ until the present time t , who will transition from E to I around the time t . Incorporating all the transitions of Eqs. (1) - (3), the SEIR dynamics take the form

$$\frac{d\mathbb{S}}{dt} = -\beta\mathbb{S}(t)\frac{\mathbb{E}(t)}{N} \quad (9)$$

$$\frac{d\mathbb{E}}{dt} = \beta\mathbb{E}(t)\frac{\mathbb{S}(t)}{N} - \mathbb{G}(t) \quad (10)$$

$$\frac{d\mathbb{I}}{dt} = \mathbb{G}(t) - \alpha\mathbb{I}(t) \quad (11)$$

$$\frac{d\mathbb{R}}{dt} = \alpha\mathbb{I}(t). \quad (12)$$

Note that infections is primarily driven by E -state individuals, as the symptomatic I individuals are isolated.

Next, we rewrite the equations for the normalized populations $S(t) = \mathbb{S}(t)/N$, $I(t) = \mathbb{I}(t)/N$, $E(t) = \mathbb{E}(t)/N$ and $R(t) = \mathbb{R}(t)/N$, capturing the fraction of individuals in each state. We arrive at our final SEIR equations

$$\frac{dS}{dt} = -\beta S(t)E(t) \quad (13)$$

$$\frac{dE}{dt} = \beta E(t)S(t) - G(t) \quad (14)$$

$$\frac{dI}{dt} = G(t) - \alpha I(t) \quad (15)$$

$$\frac{dR}{dt} = \alpha I(t), \quad (16)$$

where

$$G(t) = \int_0^t g(t')\beta S(t-t')E(t-t') dt'. \quad (17)$$

Appendix B. Modeling alternating lock-downs

To track the dynamics of COVID-19 under alternating lock-downs we first partition the population into 2 groups that alternate between the lock-down state L and the free state F. In each of these groups there is a fraction f of defectors D and $1 - f$ of cooperators C. This divides all individuals into four distinct classes: LC, LD, FC and FD, capturing the cooperators/defectors in the locked-down/free groups. We use superscript to denote an individual's class, hence, *e.g.*, $E^{LC}(t)$ represents the amount of exposed individuals who are in the lock-down group and are cooperative. These individuals will not contribute to the infection, as they comply with the stay-home instructions. Conversely, $E^{LD}(t)$ captures the defective individuals, who choose to remain active and violate the lock-down. Together with $E^{FC}(t)$ and $E^{FD}(t)$, the exposed individuals in the F group, they will contribute to spreading the virus. This results in two sets of equations. For the lock-down group L we obtain

$$\frac{dS^{LC}}{dt} = 0 \quad (18)$$

$$\frac{dE^{LC}}{dt} = - \int_0^t g(t') \beta S^{LC}(t-t') E^T(t-t') dt' \quad (19)$$

$$\frac{dI^{LC}}{dt} = \int_0^t g(t') \beta S^{LC}(t-t') E^T(t-t') dt' - \alpha I^{LC}(t) \quad (20)$$

$$\frac{dR^{LC}}{dt} = \alpha I^{LC}(t) \quad (21)$$

$$\frac{dS^{LD}}{dt} = -\beta S^{LD}(t) E^T(t) \quad (22)$$

$$\frac{dE^{LD}}{dt} = \beta S^{LD}(t) E^T(t) - \int_0^t g(t') \beta S^{LD}(t-t') E^T(t-t') dt' \quad (23)$$

$$\frac{dI^{LD}}{dt} = \int_0^t g(t') \beta S^{LD}(t-t') E^T(t-t') dt' - \alpha I^{LD}(t) \quad (24)$$

$$\frac{dR^{LD}}{dt} = \alpha I^{LD}(t), \quad (25)$$

where

$$E^T(t) = E^{LD}(t) + E^{FC}(t) + E^{FD}(t). \quad (26)$$

Infections are caused by all exposed individuals who remain active, whether officially or by defection. As explained above, the infected are always isolated, even if defective, hence all I individuals are excluded from the process of infection.

For the free group we write

$$\frac{dS^{\text{FC}}}{dt} = -\beta S^{\text{FC}}(t)E^{\text{T}}(t) \quad (27)$$

$$\frac{dE^{\text{FC}}}{dt} = \beta S^{\text{FC}}(t)\left(E^{\text{T}}(t)\right) - \int_0^t g(t')\beta S^{\text{FC}}(t-t')E^{\text{T}}(t-t') dt' \quad (28)$$

$$\frac{dI^{\text{FC}}}{dt} = \int_0^t g(t')\beta S^{\text{FC}}(t-t')E^{\text{T}}(t-t') dt' - \alpha I^{\text{FC}}(t) \quad (29)$$

$$\frac{dR^{\text{FC}}}{dt} = \alpha I^{\text{FC}}(t) \quad (30)$$

$$\frac{dS^{\text{FD}}}{dt} = -\beta S^{\text{FD}}(t)E^{\text{T}}(t) \quad (31)$$

$$\frac{dE^{\text{FD}}}{dt} = \beta S^{\text{FD}}(t)E^{\text{T}}(t) - \int_0^t g(t')\beta S^{\text{FD}}(t-t')E^{\text{T}}(t-t') dt' \quad (32)$$

$$\frac{dI^{\text{FD}}}{dt} = \int_0^t g(t')\beta S^{\text{FD}}(t-t')E^{\text{T}}(t-t') dt' - \alpha I^{\text{FD}}(t) \quad (33)$$

$$\frac{dR^{\text{FD}}}{dt} = \alpha I^{\text{FD}}(t). \quad (34)$$

To set the initial conditions we consider the response time t_0 when we employ our intervention. At this time point the state of the system is given by $S(t_0), E(t_0), I(t_0), R(t_0)$. We first partition them into two equal groups, each with a fraction f of defectors. Hence at the intervention point t_0 we have

$$\begin{aligned} S^{\text{LC}}(t_0) &= \frac{1}{2}(1-f)S(t_0), & S^{\text{LD}}(t_0) &= \frac{1}{2}fS(t_0) \\ S^{\text{FC}}(t_0) &= \frac{1}{2}(1-f)S(t_0), & S^{\text{FD}}(t_0) &= \frac{1}{2}fS(t_0) \\ E^{\text{LC}}(t_0) &= \frac{1}{2}(1-f)E(t_0), & E^{\text{LD}}(t_0) &= \frac{1}{2}fE(t_0) \\ E^{\text{FC}}(t_0) &= \frac{1}{2}(1-f)E(t_0), & E^{\text{FD}}(t_0) &= \frac{1}{2}fE(t_0) \\ I^{\text{LC}}(t_0) &= \frac{1}{2}(1-f)I(t_0), & I^{\text{LD}}(t_0) &= \frac{1}{2}fI(t_0) \\ I^{\text{FC}}(t_0) &= \frac{1}{2}(1-f)I(t_0), & I^{\text{FD}}(t_0) &= \frac{1}{2}fI(t_0) \\ R^{\text{LC}}(t_0) &= \frac{1}{2}(1-f)R(t_0), & R^{\text{LD}}(t_0) &= \frac{1}{2}fR(t_0) \\ R^{\text{FC}}(t_0) &= \frac{1}{2}(1-f)R(t_0), & R^{\text{FD}}(t_0) &= \frac{1}{2}fR(t_0). \end{aligned} \quad (35)$$

Setting the initial condition according to Eq. (35) we solve Eqs. (18) - (34) for a period of 7 days. We then switch between the L and F groups, setting $S^{\text{LC}}(t) = S^{\text{FC}}(t), E^{\text{LC}}(t) = E^{\text{FC}}(t) \dots$ and vice versa, proceeding to solve the equations for an additional 7 days. We continue with such weekly iterations, until we reach steady-state where $I(t \rightarrow \infty) \rightarrow 0$.